presented using the Psychophysics Toolbox (www.psychtoolbox.org) under Matlab (Mathworks). Stimuli were projected for 1 s onto a back-projection screen using an LCD projector (Sharp). Subjects decided whether an image was a face or a house and responded with a button press after a forced delay, which was included to make the task as analogous to the studies in monkeys as possible (those experiments typically include a forced delay[1]) (compare Fig. 1c). The sequence of events was optimized using rsfgen (AFNI, http://afni.nimh.nih.gov).

Data acquisition and analysis

Whole-brain MRI data were collected on a 3T GE Signa (GE Medical Systems). Echoplanar data were acquired using standard parameters (Field of view, 200 mm; matrix, 64 × 64; 25 axial slices, 5 mm thick; in-plane resolution, 3.125 mm; repetition time, TR, 2.0 s; error time, TE, 30 ms; flip angle, 90°). Five to eight runs of 162 volumes each were acquired. The first four volumes were discarded to allow for magnetization equilibration. To minimize head motion, we used both a bite bar and a vacuum head pad. A T1 weighted volume (MP-RAGE) was acquired for anatomical comparison.

MRI data were analysed using a mixed effects approach within the framework of the general linear model (GLM as implemented in FSL 5.0, http://www.fmrib.ox.ac.uk/fsl). Pre-processing was applied: slice-time correction, motion correction, non-brain removal, spatial smoothing using a kernel of 8 mm full-width at half-maximum, mean-based intensity normalization of all volumes by the same factor; highpass temporal filtering (gaussian-weighted least-squares straight line fitting, with sigma = 50.0 s). Time-series statistical analysis was carried out using FSL with local autocorrelation correction[29]. Trials in which subjects gave no response or an incorrect response were pooled together and modelled as a regressor of no interest (error trials). Hence, similar to the studies in monkeys, only correct trials were used to model regressors for the four conditions (suprathreshold face, perithreshold face, perithreshold house and suprathreshold house). The average number of trials was 215.5 ± 29.7 (mean ± s.d.) for suprathreshold face, 190.17 ± 31.6 for perithreshold face, 194.7 ± 30.8 for perithreshold house and 202.8 ± 26.8 for suprathreshold house, respectively. Time series were modelled using event-related regressors for each of the four conditions as well as error trials, and convolved with the haemodynamic response function (gamma variate). Contrast images for each condition and the contrasts of interest for each subject were computed and transformed, after spatial normalization, into standard (MNI152) space. Group effects were computed using the transformed contrast images in a mixed effects model treating subjects as random. The resulting Z statistic images were thresholded at $Z > 3.1$, corresponding to $P < 0.001$, uncorrected. For display purposes, statistic images are shown with $Z > 2.6$, corresponding to $P < 0.005$. In each subject we determined voxels in the temporal cortex that were more responsive to faces than to houses, and vice versa. The region analysed included the lingual, parahippocampal, fusiform and inferior temporal gyri 70 to 20 mm posterior to the anterior commissure in Talairach brain atlas coordinates (see ref. 30). To test in which voxels the BOLD signal significantly covaried with $|\mathrm{Face}(t) - \mathrm{House}(t)|$, we set up an additional model using the following three regressors: (1) the difference between the regressors for the suprathreshold and the perithreshold conditions used in the GLM analysis described above ((suprathreshold face + suprathreshold house) − (perithreshold face + perithreshold house)); (2) the absolute difference between the time series in face- and house-responsive voxels in each subject ($|\mathrm{Face}(t) - \mathrm{House}(t)|$); and (3) the product of the first and second regressors, representing the interaction between ($|\mathrm{Face}(t) - \mathrm{House}(t)|$) (physiological signal) and task-related parameters (psychological factor, hence psychophysiological interaction). Contrast images and group effects were computed as described above. We did not find any voxels in which changes in activity significantly covaried with the psychophysiological interaction term.

Received 13 April; accepted 24 August 2004; doi:10.1038/nature02966.

1. Shadlen, M. N. & Newsome, W. T. Neural basis of a perceptual decision in the parietal cortex (area LIP) of the rhesus monkey. *J. Neurophysiol.* **86,** 1916–1936 (2001).
2. Kim, J. N. & Shadlen, M. N. Neural correlates of a decision in the dorsolateral prefrontal cortex of the macaque. *Nature Neurosci.* **2,** 176–185 (1999).
3. Gold, J. I. & Shadlen, M. N. Neural computations that underlie decisions about sensory stimuli. *Trends Cogn. Sci.* **5,** 10–16 (2001).
4. Ditterich, J., Mazurek, M. E. & Shadlen, M. N. Microstimulation of visual cortex affects the speed of perceptual decisions. *Nature Neurosci.* **6,** 891–898 (2003).
5. Newsome, W. T., Britten, K. H. & Movshon, J. A. Neuronal correlates of a perceptual decision. *Nature* **341,** 52–54 (1989).
6. Salzman, C. D., Britten, K. H. & Newsome, W. T. Cortical microstimulation influences perceptual judgements of motion direction. *Nature* **346,** 174–177 (1990).
7. Schall, J. D. Neural basis of deciding, choosing and acting. *Nature Rev. Neurosci.* **2,** 33–42 (2001).
8. Romo, R. & Salinas, E. Flutter discrimination: neural codes, perception, memory and decision making. *Nature Rev. Neurosci.* **4,** 203–218 (2003).
9. Shadlen, M. N., Britten, K. H., Newsome, W. T. & Movshon, J. A. A computational analysis of the relationship between neuronal and behavioral responses to visual motion. *J. Neurosci.* **16,** 1486–1510 (1996).
10. Romo, R., Hernandez, A., Zainos, A. & Salinas, E. Correlated neuronal discharges that increase coding efficiency during perceptual discrimination. *Neuron* **38,** 649–657 (2003).
11. Hernandez, A., Zainos, A. & Romo, R. Temporal evolution of a decision-making process in medial premotor cortex. *Neuron* **33,** 959–972 (2002).
12. Haxby, J. V. *et al.* The functional organization of human extrastriate cortex: a PET-rCBF study of selective attention to faces and locations. *J. Neurosci.* **14,** 6336–6353 (1994).
13. Kanwisher, N., McDermott, J. & Chun, M. M. The fusiform face area: a module in human extrastriate cortex specialized for face perception. *J. Neurosci.* **17,** 4302–4311 (1997).
14. McCarthy, G., Puce, A., Gore, J. C. & Allison, T. Face-specific processing in the human fusiform gyrus. *J. Cogn. Neurosci.* **9,** 605–610 (1997).
15. Epstein, R. & Kanwisher, N. A cortical representation of the local visual environment. *Nature* **392,** 598–601 (1998).
16. Ishai, A., Ungerleider, L. G., Martin, A., Schouten, J. L. & Haxby, J. V. Distributed representation of objects in the human ventral visual pathway. *Proc. Natl Acad. Sci. USA* **96,** 9379–9384 (1999).
17. Logothetis, N. K., Pauls, J., Augath, M., Trinath, T. & Oeltermann, A. Neurophysiological investigation of the basis of the fMRI signal. *Nature* **412,** 150–157 (2001).
18. Logothetis, N. K. & Wandell, B. A. Interpreting the BOLD Signal. *Annu. Rev. Physiol.* **66,** 735–769 (2004).
19. Corbetta, M. & Shulman, G. L. Control of goal-directed and stimulus-driven attention in the brain. *Nature Rev. Neurosci.* **3,** 201–215 (2002).
20. Pessoa, L., Kastner, S. & Ungerleider, L. G. Neuroimaging studies of attention: from modulation of sensory processing to top-down control. *J. Neurosci.* **23,** 3990–3998 (2003).
21. Petrides, M., Alivisatos, B., Evans, A. C. & Meyer, E. Dissociation of human mid-dorsolateral from posterior dorsolateral frontal cortex in memory processing. *Proc. Natl Acad. Sci. USA* **90,** 873–877 (1993).
22. Koechlin, E., Ody, C. & Kouneiher, F. The architecture of cognitive control in the human prefrontal cortex. *Science* **302,** 1181–1185 (2003).
23. Petrides, M. Deficits in non-spatial conditional associative learning after periarcuate lesions in the monkey. *Behav. Brain Res.* **16,** 95–101 (1985).
24. Miller, E. K. & Cohen, J. D. An integrative theory of prefrontal cortex function. *Annu. Rev. Neurosci.* **24,** 167–202 (2001).
25. Platt, M. L. & Glimcher, P. W. Neural correlates of decision variables in parietal cortex. *Nature* **400,** 233–238 (1999).
26. Sharma, J., Dragoi, V., Tenenbaum, J. B., Miller, E. K. & Sur, M. V1 neurons signal acquisition of an internal representation of stimulus location. *Science* **300,** 1758–1763 (2003).
27. Sugrue, L. P., Corrado, G. S. & Newsome, W. T. Matching behavior and the representation of value in the parietal cortex. *Science* **304,** 1782–1787 (2004).
28. Rainer, G. & Miller, E. K. Effects of visual experience on the representation of objects in the prefrontal cortex. *Neuron* **27,** 179–189 (2000).
29. Woolrich, M. W., Ripley, B. D., Brady, M. & Smith, S. M. Temporal autocorrelation in univariate linear modeling of FMRI data. *Neuroimage* **14,** 1370–1386 (2001).
30. Haxby, J. V. *et al.* Distributed and overlapping representations of faces and objects in ventral temporal cortex. *Science* **293,** 2425–2430 (2001).
31. Heekeren, H. R., Marrett, S., Bandettini, P. A. & Ungerleider, L. G. Neural correlates of a decision in human dorsolateral prefrontal cortex. *Soc. Neurosci. Abs* Program No. 16.3 (2002); ⟨http://sfn.scholarone.com/itin2002/main.html?new_page_id=126&abstract_id=13054&p_num=16.3&is_tech=020.01.2004%2006:24:56⟩.

Supplementary Information accompanies the paper on **www.nature.com/nature.**

Acknowledgements We thank D. Ruff and I. Wartenburger for technical help and manuscript preparation, and M. Beauchamp, R. Desimone, A. Ishai and A. Martin for comments on the manuscript. This study was supported by the National Institute of Mental Health (NIMH) Intramural Research Program, the Deutsche Forschungsgemeinschaft (DFG, Emmy Noether Programme) and the Bundesministerium für Bildung und Forschung (BMBF, Berlin NeuroImaging Center).

Competing interests statement The authors declare that they have no competing financial interests.

Correspondence and requests for materials should be addressed to H.R.H. (hauke@nih.gov).

Coupled oscillators control morning and evening locomotor behaviour of *Drosophila*

Dan Stoleru*, Ying Peng*, José Agosto & Michael Rosbash

Howard Hughes Medical Institute and National Center for Behavioural Genomics, Department of Biology, Brandeis University, Waltham, Massachusetts 02454, USA

* These authors contributed equally to this work

Daily rhythms of physiology and behaviour are precisely timed by an endogenous circadian clock[1,2]. These include separate bouts of morning and evening activity, characteristic of *Drosophila melanogaster* and many other taxa, including mammals[3–5]. Whereas multiple oscillators have long been proposed to orchestrate such complex behavioural programmes[6], their nature and interplay have remained elusive. By using cell-specific ablation, we show that the timing of morning and evening activity in

***Drosophila* derives from two distinct groups of circadian neurons: morning activity from the ventral lateral neurons that express the neuropeptide PDF, and evening activity from another group of cells, including the dorsal lateral neurons. Although the two oscillators can function autonomously, cell-specific rescue experiments with circadian clock mutants indicate that they are functionally coupled.**

Circadian rhythms arose during evolution, by adapting to and then anticipating the 24-h rotation of the Earth and its consequent light/dark cycle[1,2]. During a generic day of 12 h of daylight followed by 12 h of darkness (LD), wild-type *D. melanogaster* flies exhibit two distinct bouts of locomotor activity: one is centred at dawn (morning) and the other at dusk (evening), similar to many crepuscular insect species. The morning and evening activity peaks begin before lights-on and lights-off, respectively, indicating that flies anticipate the discontinuous morning (dark to light) and evening (light to dark) transitions that take place under LD conditions. Although there are some indications that the morning peak may not require all of the canonical oscillator components[3,7], there is other evidence that the morning as well as the evening anticipation requires an endogenous circadian oscillator[4,5,7]. For example, a number of arrhythmic mutants fail to ramp-up their activity during the last 2–3 h of daytime and night time; instead they exhibit driven periodic behaviour, consisting of abrupt activity elevations (startle responses) immediately after lights-on and lights-off[3].

There are approximately 100 circadian clock neurons, bilaterally clustered in six defined groups of cells within the adult fly brain[8]. Two of these regions, the small and large ventral lateral neurons (LN_vs), express the neuropeptide PDF (also referred to hereafter as PDF^+ or PDF-expressing cells) and make an important contribution to circadian locomotor activity rhythms[9–11]. Ablation of these cells by targeted expression of proapoptotic genes causes arrhythmicity in DD conditions[10]. Our recent study indicated that the LN_vs are key cellular coordinators that synchronize or maintain rhythmic gene expression within the circadian network[12]. However, ablation of the LN_vs affects only limited aspects of behavioural rhythms under LD conditions[10], indicating that there are other important cellular substrates that control circadian behaviour under natural conditions.

To identify these additional circadian clock cells, we sought to assay locomotor activity in a strain ablated of more clock neurons

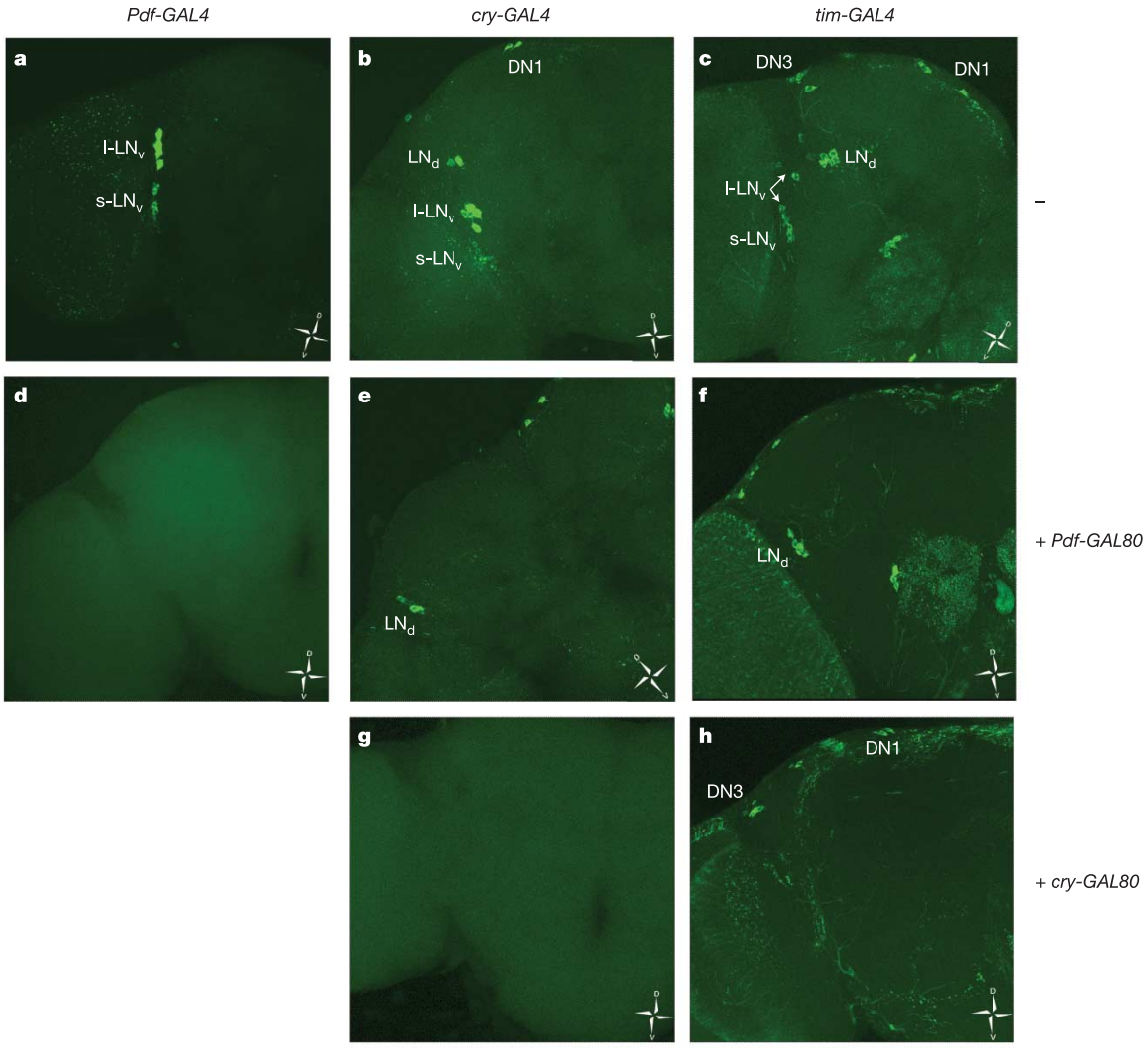

Figure 1 Suppression of *GAL4* activity with *GAL80* in *Drosophila* circadian neurons, as examined with a *UAS-ANFGFP* reporter. **a**–**c**, *GAL4* only. **a**, *Pdf-GAL4*-targeted expression in LN_vs[11]. **b**, *cry-GAL4* in LN_vs, LN_ds and two DN1 cells[13–15]. **c**, *tim-GAL4* (ref. 8) in all circadian neuronal groups. **d**–**f**, *Pdf-GAL80* suppresses *GAL4* activation in the LN_vs. **d**, *Pdf-GAL4; Pdf-GAL80; UAS-ANFGFP*. **e**, *cry-GAL4; Pdf-GAL80; UAS-ANFGFP*. **f**, *tim-GAL4; Pdf-GAL80; UAS-ANFGFP*. **g**, **h**, *cry-GAL80* suppresses *GAL4* in a wider group of neurons. **g**, *cry-GAL4; cry-GAL80; UAS-ANFGFP*. **h**, *tim-GAL4; cry-GAL80; UAS-ANFGFP*. In each panel a compass rose indicates the orientation of the brain (D, dorsal; V, ventral). See Supplementary Table S1 for further details.

than just the LN_vs. The *tim-GAL4* transgene drives gene expression ubiquitously in all six groups of clock cells[8]; that is, in the three groups of dorsal neurons (DN1, DN2, DN3), the dorsal-lateral neurons (LN_ds) as well as the two groups of PDF-expressing LN_vs. However, targeted expression of the proapoptotic gene *hid* with the *tim-GAL4* driver led to embryonic lethality, precluding any assay of locomotor activity. The circadian photoreceptor *cryptochrome* (*cry*) gene is expressed in many circadian neurons of the adult brain[13,14],

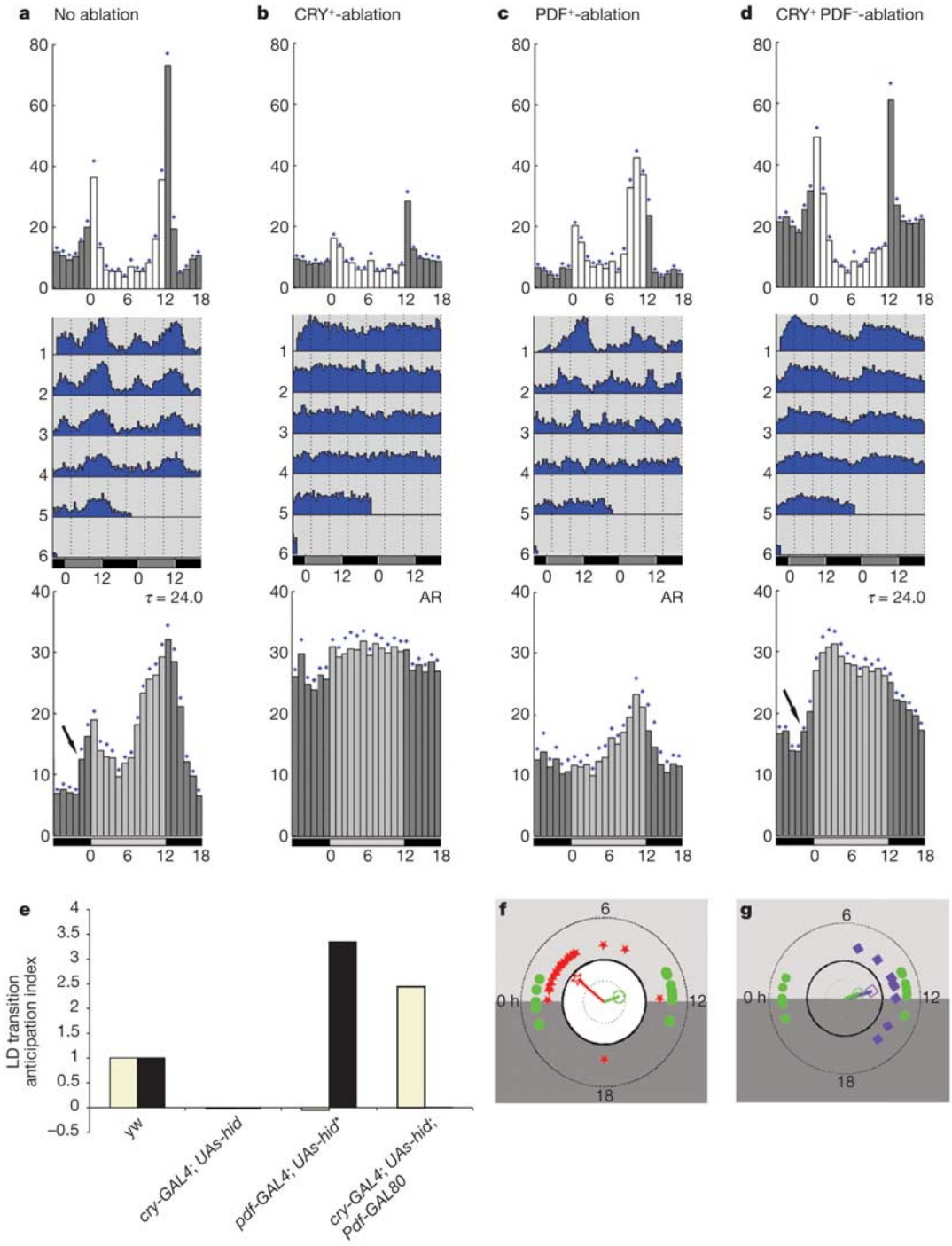

Figure 2 Genetic ablation of different groups of circadian neurons causes the loss of different locomotor activity components. **a**–**d**, Comparison of the circadian locomotor behaviour of normal rhythm (*y w*) flies (**a**) with that of transgenic flies with different circadian neurons ablated (**b**–**d**). Top panels, group LD activity in histogram format; middle panels, double-plotted actograms of group DD activity; bottom panels, the same group DD activities plotted as histograms. In the histograms, the lighting condition is indicated by the colour of the activity bin (LD: white = day and dark grey = night; DD: light grey = subjective day and dark grey = subjective night). The blue diamonds indicate the standard error of the mean. **a**, *y w* flies; **b**, [CRY^+]-ablated flies (*cry-GAL4*; *UAS-hid*); **c**, [PDF^+]-ablated flies (*Pdf-GAL4*; *UAS-hid*); **d**, [CRY^+PDF^-]-ablated flies (*cry-GAL4*; *Pdf-GAL80*; *UAS-hid*). **e**, Summary of LD lights-on and lights-off anticipation for wild type and for the three ablation genotypes (see Methods for the normalized AI). Asterisk, evening anticipation of [PDF^+]-ablated flies, shifted 1 h[10]. Yellow columns indicate mornings and black columns indicate evenings. **f**, **g**, Circular phase analysis of DD locomotor activity for individual flies. The green circles represent phase estimates for *y w* flies. **f**, [CRY^+PDF^-]-ablated flies (*cry-GAL4*; *Pdf-GAL80*; *UAS-hid*; red stars). **g**, [PDF^+]-ablated flies (*Pdf-GAL4*; *UAS-hid*; blue squares). The timing is shown in CT hours. Subjective day (CT0-12) is in light grey whereas subjective night (CT12-24) is dark grey. See Supplementary Table S4 for further details.

much more broadly than *Pdf*. On the basis of the supposition that these light-sensing neurons may have a prominent role in controlling LD rhythms, we focused on a previously characterized *cry-GAL4* driver (*cry*$_{13}$*-GAL4*)[13] that induces expression in the LN_v and LN_d cells (Fig. 1b)[13]. To clarify an inconsistency in the previous description of this driver[15], we used a stronger green fluorescent protein (GFP) reporter[16]. The large LN_vs were the most prominently stained cells, and all lateral neurons (that is, LN_vs and LN_ds) were GFP-positive. We also observed consistent GFP expression in two additional locations: two very dorsal DN1 cells (Fig. 1b, e) and the one PDF-negative LN_v cell[17] (Supplementary Table S1). The most dorsally positioned pair of adult DN1 cells was recently shown to express high levels of CRY, lack expression of Glass protein and correspond to the two larval DN1 cells[14]. Although CRY is probably even more widely expressed[14], we interpret this pattern of LN_vs, LN_ds and 2 DN1 cells to reflect circadian neurons with particularly high *cry* expression, and will refer to these cells as CRY^+.

The pattern of LD locomotor activity for *cry-GAL4*; *UAS-hid* flies (which are viable and morphologically normal) was conspicuously different from that of wild-type (Fig. 2a, top panel) and of LN_v-ablated flies (*Pdf-GAL4*; *UAS-hid*, Fig. 2c, top panel) and is one of the most severe circadian defects known so far: there is no anticipation of either lights-on or lights-off (Fig. 2b, top panel). In DD, the *cry-GAL4*; *UAS-hid* strain is also completely arrhythmic (Fig. 2b, middle and bottom panels). Although this does not exclude an important role for the dorsal neurons in persistent oscillator function and entrainment[14,18], most of the dorsal neurons (which survive the ablation; Fig. 3b) are apparently incapable of driving circadian behaviour alone. We also hypothesized that the marked difference between the *cry-GAL4* ablation and the *Pdf-GAL4* ablation is due to the additional CRY-expressing cells in the former (that is, at least the LN_ds, the two DN1 cells and the PDF^- LN_v). We will henceforth refer to these cells collectively as CRY^+PDF^-.

To study the function of the CRY^+PDF^- cells and their interaction with the PDF-expressing cells, we developed a novel ternary expression system to refine the spatial resolution of clock cell targeting. On the basis of the MARCM system[19], we generated transgenic strains that express *GAL80* under the control of the *Pdf* and *cry* promoters[11,13]. To assay the suppression of *GAL4*-mediated transcriptional activation, we crossed the *GAL80* strains to flies expressing GFP in specific clock cells, under various *GAL4* drivers. *Pdf-GAL4*; *UAS-ANFGFP*; *Pdf-GAL80* and *cry-GAL4*; *UAS-ANFGFP*; *cry-GAL80* have no detectable GFP signal in the brain, suggesting that the repressive activities of *Pdf-GAL80* and *cry-GAL80* are sufficient to counteract the transcriptional activity of their respective *GAL4* drivers (Fig. 1d, g; see also Supplementary Table S1). When the *cry-GAL4* driver is combined with *Pdf-GAL80* repressor (*cry-GAL4*; *UAS-ANFGFP*; *Pdf-GAL80*, Fig. 1e; see also Supplementary Table S1), consistent GFP signal is restricted to the LN_ds, the two DN1 cells and one LN_v cell (probably the PDF^- s-LN_v cell); this is as predicted by the difference in the two promoters (Fig. 1a, b). When the pan-clock-cell *tim-GAL4* driver is combined with the *Pdf-GAL80* repressor, the expression pattern recapitulates the described *tim-GAL4* pattern with the exception of the LN_vs (Fig. 1f). The *tim-GAL4*; *cry-GAL80* combination excludes GFP signal from the LN_ds and the LN_vs (Fig. 1h; see also Supplementary Table S1).

We also assayed the efficiency of *GAL80* suppression through the use of a behavioural readout. In both cases, the *GAL80* transgenes fully rescued the behavioural defect caused by the corresponding *GAL4*-mediated cell ablation (Supplementary Tables S2 and S3). As an extra precaution, we chose two of the most potent lines expressing *Pdf-GAL80* and *cry-GAL80* and generated double insert recombinants (*Pdf-GAL80*$_{96A}$ and *cry-GAL80*$_{2e3m}$, respectively; Supplementary Tables S2 and S3), which were used in all subsequent experiments.

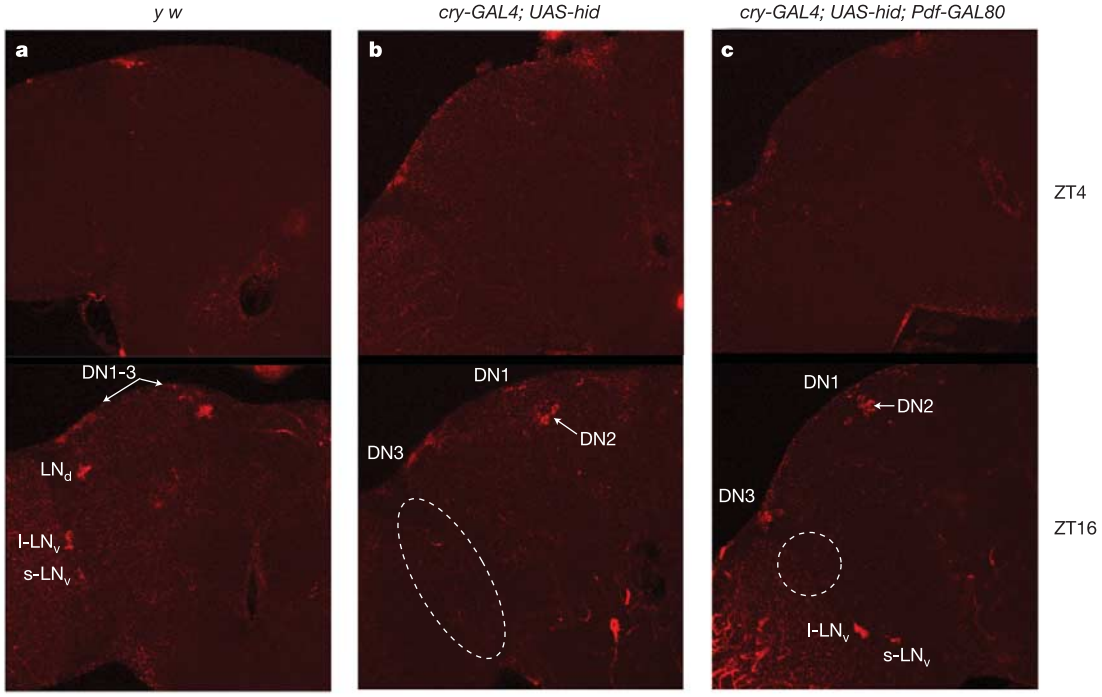

Figure 3 Targeted genetic ablation removes specific circadian neurons. Cell-specific ablation in the brain was confirmed by whole-mount *in situ* hybridization with a *tim* probe. **a**, In *y w* flies, all circadian neurons show robust *tim* oscillation between ZT4 (top) and ZT16 (bottom). ZT, Zeitgeber time, defines the timing of the LD experiment: ZT0 = the time of lights on, whereas ZT12 = the time of the lights off event. **b**, In *cry-GAL4*; *UAS-hid* flies, both LN_v and LN_d neurons are missing (dashed circles), whereas most DN cells survive the ablation and oscillate indistinguishably from wild type. **c**, In *cry-GAL4*; *Pdf-GAL80*; *UAS-hid* flies, the LN_d neurons are missing (dashed circles), whereas the LN_vs and DN cells oscillate like wild type. See 'Imaging techniques' in Methods for details.

To ablate specifically the CRY^+PDF^- cells, we crossed *Pdf-GAL80* with *cry-GAL4*; *UAS-hid* and generated progeny carrying all three transgenes (*cry-GAL4*; *Pdf-GAL80; UAS-hid*). *tim in situ* hybridizations confirmed the specific ablation of these cells (Fig. 3c). This triple transgenic strain allowed a behavioural comparison of the ablation of these three sets of neurons: PDF^+, CRY^+PDF^- and CRY^+ (Fig. 2; see also Supplementary Table S4).

The LD behaviour of the $[CRY^+PDF^-]$-ablated flies (Fig. 2d, top) appeared to be intermediate between the complete loss-of-rhythm phenotype of the $[CRY^+]$-ablated flies (Fig. 2b, top) and the largely normal phenotype of the $[PDF^+]$-ablated flies (Fig. 2c, top). On closer inspection, however, we noticed that the $[CRY^+PDF^-]$-ablated flies showed suppressed evening activity before lights-off (Fig. 2d, top panel, and e). The residual evening peak occurs after

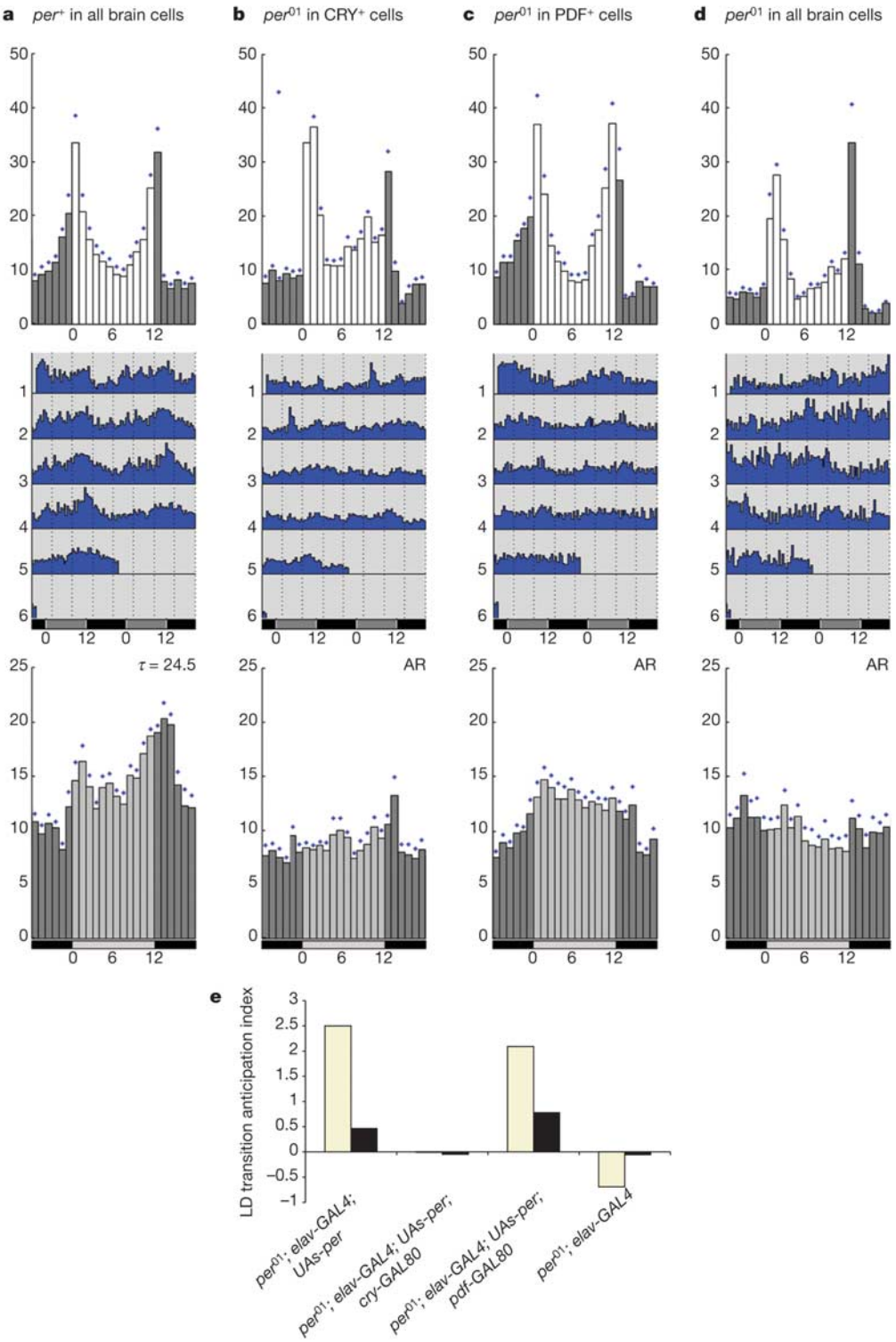

Figure 4 Functional disruption of the two oscillators. The panels are as in Fig. 2. **a**, per^{01} rescue in all of the brain neurons (per^{01}; *elav-GAL4*; *UAS-per*). **b**, Suppression of rescue in CRY^+ neurons (per^{01}; *elav-GAL4*; *UAS-per; cry-GAL80*). **c**, Suppression of rescue in PDF neurons (per^{01}; *elav-GAL4*; *UAS-per2-4; Pdf-GAL80*). **d**, Non-rescued per^{01} control (per^{01}; *elav-GAL4*). **e**, Group anticipation indices for the genotypes analysed in **a**–**d** (as in Fig. 2e). See Supplementary Table S5 for further details.

lights-off and almost certainly reflects an evening startle response, with little or no bona fide circadian anticipation[3]. In contrast, there was a robust morning peak with normal circadian anticipation of lights-on (Fig. 2d, top panel, and e). The absence of lights-off anticipation was reminiscent of the diminished morning activity peak reported in [PDF$^+$]-ablated flies or in the *Pdf*^{01} (PDF-null) mutant strain[10]. We checked the LD activity pattern of these genotypes and confirmed that they lack lights-on anticipation (Fig. 2c, e, and data not shown). The results indicate that the CRY$^+$PDF$^-$ cells govern the evening activity peak, whereas the PDF-expressing cells govern the morning activity peak; these two oscillators can function independently.

The behaviour of these strains in DD does not differ from LD, which verifies our conclusions and confirms that neither activity peak is driven by light (Fig. 2a–d, middle and bottom panels). In contrast to the [PDF$^+$]-ablation (in which the locomotor activity rhythm damps down during the first few days in DD; Fig. 2c, middle panel) and the [CRY$^+$]-ablation (which abolishes rhythmicity; Fig. 2b), the [CRY$^+$PDF$^-$]-ablation is characterized by a robust and sustained rhythm in DD with a wild-type period ($\tau = 24.0$ h; Fig. 2d). However, these [CRY$^+$PDF$^-$]-ablated flies have a unimodal, apparently morning-only activity pattern (Fig. 2d, bottom). The timing of the morning locomotor activity increase is indistinguishable from that of wild type (Fig. 2a, d, arrows), but [CRY$^+$PDF$^-$]-ablated flies fail to suppress strongly the activity after subjective morning. This prolonged activity bout delays the calculated phase by more than 2 h relative to the phase of wild-type morning activity (Fig. 2f; see also Supplementary Table S4)[3]. The absence of a robust DD evening activity bout in the [CRY$^+$PDF$^-$]-ablated flies confirms the importance of these cells for this aspect of locomotor output (Fig. 2d). [PDF$^+$]-ablated flies as well as the *Pdf*^{01} mutant strain also have a predominantly unimodal locomotor activity pattern that corresponds to subjective evening[10] (Fig. 2c, g, and data not shown). Although these flies are only weakly rhythmic during the first few days of DD, the absence of a morning peak is evident[10] (Fig. 2e, g) and confirms the importance of the PDF-expressing cells for this aspect of the activity programme. We propose that these two oscillators generate distinct output signals to govern the morning and evening activity peaks, respectively. Because the *Pdf*^{01} mutant is missing the morning peak yet retains intact transcriptional oscillations in the LN$_v$s under LD conditions[12], the PDF peptide is a strong candidate for the morning output signal from the LN$_v$s.

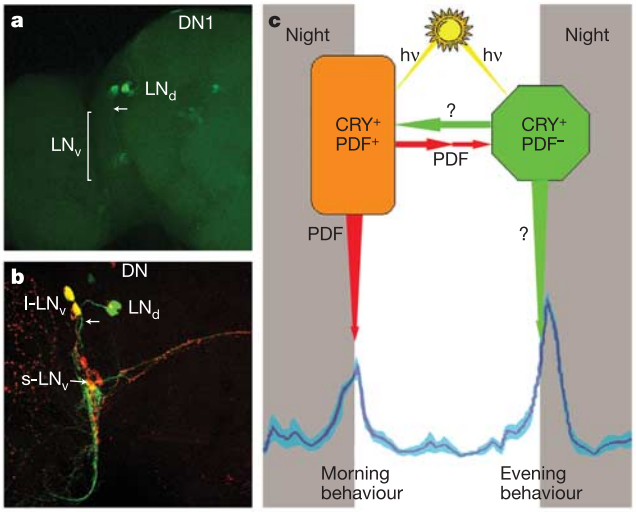

Figure 5 Coupling of the two *Drosophila* oscillators CRY$^+$PDF$^-$ and PDF$^+$ underlies the coordination of the two daily activity peaks. **a**, CRY$^+$PDF$^-$ cells project neurites onto the LN$_v$ region, visualized here with a membrane-labelling GFP reporter (green; *cry-GAL4*; *Pdf-GAL80*; *UAS-mCD8iGFP*). **b**, PDF immunostaining (red) of *cry-GAL4*; *UAS-mCD8iGFP* adult brains shows that CRY$^+$PDF$^-$ cells send a PDF$^-$ axonal process (green, arrow) towards the region of PDF$^+$ cells (LN$_v$s, in red). The red dots localized in the LN$_d$ and DN regions might indicate a reciprocal connection (PDF peptide released from LN$_v$ terminals). **c**, Model of the circadian network responsible for morning and evening activity in *Drosophila*. PDF$^+$ and CRY$^+$PDF$^-$ cells function as morning and evening oscillators, respectively. A wild-type diel activity plot is shown in blue. hν indicates the action of light.

The notion of differentially timed outputs is based on the synchrony of the circadian programmes within the CRY$^+$ cells; that is, the indistinguishable phase of molecular oscillation within all clock neurons in the brain as indicated by *in situ* hybridization[12,15] or immunohistochemistry[8]. On the basis of our recent evidence indicating that clock cells constitute a network[12], we used another strategy to examine the autonomy of the CRY$^+$PDF$^-$ and PDF$^+$ cells and selectively disrupted their molecular oscillations. *per*^{01} is a canonical circadian mutant that eliminates the Period protein (PER) and causes the loss of both molecular and behavioural rhythmicity[20]. A *UAS-per* transgene (*UAS-per2-4*), driven by the pan-neuronal *elav-GAL4* driver (*elav*^{C155}*-GAL4*), was previously used to rescue the behavioural defect of *per*^{01} (ref. 21). We verified this result (Fig. 4a; see also Supplementary Table S5) and then introduced *cry-GAL80* into this system to block rescue in the CRY$^+$ cells. The resulting genotype (*per*^{01}; *elav-GAL4*; *UAS-per; cry-GAL80*) was completely arrhythmic (AR) in DD (Fig. 4b, bottom panel) and in LD (Fig. 4b, top panel, and e) conditions. This mimics the behavioural phenotype of [CRY$^+$]-ablated flies and verifies that both activity peaks are predominantly clock-regulated. We also introduced *Pdf-GAL80* instead of *cry-GAL80* into the system to block rescue of *per*^{01} only in the PDF-expressing cells (*per*^{01}; *elav-GAL4*; *UAS-per; Pdf-GAL80*). The block was effective because the flies became gradually arrhythmic under DD conditions (Fig. 4c, middle and bottom panels), and mimicked the phenotype of [PDF$^+$]-ablated or *Pdf*^{01} flies[10].

The LD behaviour of these LN$_v$-*per*^{01} flies, however, was unexpected: they manifested a wild-type-like anticipation of lights-on as well as lights-off (Fig. 4c, f), as opposed to [PDF$^+$]-ablated flies, which only have a lights-off (evening) peak in LD (Fig. 2e). As anticipation of morning is a characteristic of a functional LN$_v$ clock, we interpret the lights-on peak to indicate the recovery of at least PDF output function. As the *cry-GAL80*-blocked flies are arrhythmic and show essentially no anticipation (Fig. 4c, e), this recovery of a morning peak requires a functional oscillator within the CRY$^+$PDF$^-$ cells. These evening peak CRY$^+$PDF$^-$ cells can apparently drive the clockless PDF neurons to direct a seemingly normal morning peak under LD conditions.

Pittendrigh and Daan proposed the existence of two circadian oscillators to explain the morning and evening activity peaks characteristic of diurnal behaviour in many species[6]. Our genetic dissection of the *Drosophila* circadian system shows that there are indeed two oscillators, which are located in two distinct cell groups. They can act independently and control these two canonical features of the wild-type behavioural programme: the PDF$^+$ cells drive the morning activity peak, and the CRY$^+$PDF$^-$ neurons drive the evening peak (Fig. 5). The latter may be specialized daytime cells, because the evening peak begins in the middle of the light period. Similarly, the PDF$^+$ cells may be night time cells. This also fits with the importance of the PDF-expressing cells for rhythmicity in constant darkness[10,12].

Although a comparable functional dissection of the mammalian circadian system has not been reported, different portions of the suprachiasmatic nuclei (SCN) probably control different aspects of the circadian programme[22,23]. Indeed, the left and right SCN may constitute separable oscillators[24]. Recent results also show that clocks in different SCN subregions have different phases[25]. Although this possibility needs to be examined more carefully in

flies, there is at present no evidence for significant phase differences between the six groups of adult brain neurons. This is consistent with the notion that the morning and evening outputs from the two relevant cell groups connect independently to the same core oscillator mechanism. Although we cannot functionally distinguish between the few $CRY^{+}PDF^{-}$ cells (that is, the LN_ds, the two DN1 cells and the single PDF^{-} small LN_v) or between the more weakly expressing clock cells, we favour the LN_ds as the evening cell group, because of efferent projection from the LN_ds to the LN_v region (Fig. 5a, b). Finally, recent evidence suggests that LN_vs on the one hand and some more dorsal neurons (LN_ds and some DN cells) on the other can constitute distinct oscillators under some conditions[26].

Functional restoration of the morning activity peak in per^{01} PDF^{+} cells could occur by driving oscillator function or by driving the output without rescuing the intracellular oscillator itself. Although previous work has suggested that intercellular communication can help maintain robust intracellular oscillations in both flies and mammals[12,25,27,28], similar studies have not been done in the context of a defective oscillator. It will therefore be important to determine which aspects of the molecular programme can be externally driven in the absence of a key endogenous clock component. In any case, it is likely that coupling of the two *Drosophila* oscillators coordinates the two major activity peaks and facilitates a response to environmental challenges such as seasonal changes. Complex intercellular regulation probably accounts for the evolution of even more complicated circadian systems such as the mammalian SCN.

Note added in proof: While this manuscript was in review, we learned that F. Rouyer and colleagues[31] had carried out similar experiments and reached almost identical conclusions, namely that the LN_ds drive the evening activity peak and the LN_vs the morning peak. □

Methods

Drosophila genetics

The *GAL80* open reading frame and SV40 poly A sequence was amplified by polymerase chain reaction (PCR) from tubulinP-*GAL80* (ref. 19) and subcloned in pBluescript SK vectors under *Pdf* 2.4-kilobase (kb)[11] and *cry* 5.5-kb[13] promoters, respectively. The fused *Pdf-GAL80* and *cry-GAL80* constructs were excised and cloned into pCaSpeR3 vector between *Sac*II and *Xho*I (*Pdf-GAL80*), and *Bam*HI and *Xho*I (*cry-GAL80*). The transformation plasmids were used to generate transgenic flies through standard embryo microinjection procedures. Eleven *Pdf-GAL80* and twenty *cry-GAL80* lines were obtained (Supplementary Tables S2 and S3). Recombinant chromosomes bearing multiple copies of each transgene were generated and verified for their ability to suppress *GAL4* transcription. In all the presented experiments, the *GAL80* strains used ($Pdf\text{-}GAL80_{96A}$ and $cry\text{-}GAL80_{2e3m}$) carried two inserts of the respective *GAL80* transgenes. *UAS-per2-4* transgenic flies[21] were provided by A. Sehgal and *UAS-ANFGFP* (ref. 16) flies by E. Levitan.

Behavioural analysis

Flies were entrained for 3 days in 12 h light/12 h dark (LD) conditions before initiating an LD experiment and for at least 5 days for each DD experiment. Locomotor activities of individual flies were monitored using Trikinetics *Drosophila* activity monitors. The analysis was done with a signal processing toolbox[29] implemented in MATLAB (MathWorks). Autocorrelation and spectral analysis were used to assess rhythmicity and to estimate period. The phase information was obtained by using circular statistics[30]. A low-pass butterworth filter was applied to detect the less robust subjective morning peak of wild-type flies. The anticipation index ($AI = b_{-1}(b_{-1} - b_{-2})(b_{-2} - b_{-3})/b_{+1}$) was developed to reflect the fact that anticipation of light transition is directly proportional to the gradual increase in activity before the transition ($(b_{-1} - b_{-2})\ (b_{-2} - b_{-3})$) and inversely proportional to the startle effect (b_{+1}/b_{-1}), where b_i = activity counts in bin i, and i = number of bin before (−i) and after (+i) light switch. Finally, the morning and evening anticipation index of each genotype was normalized to that of wild type ($AI_{yw} = 1$). Other methods of measuring the anticipation gave similar results (data not shown).

Imaging techniques

Fly brains were dissected and mounted as previously described[12]. *In situ* hybridization of *tim* has also been described[15]. At least 15 brains were examined for each time and genotype in two independent experiments, with indistinguishable results (Fig. 3). The *in situ* experiment shown in Fig. 3c was carried out four independent times, with identical results. For immunodetection of PDF, adult fly brains were incubated with rabbit anti-PDF (dilution 1:5,000). Donkey anti-rabbit IgG (TexasRed-conjugated, Jackson ImmunoResearch) was used at 1:200 dilution. A Leica laser-scanning confocal microscope was used to obtain optical sections of 1–1.2-μm thickness, which were used to construct maximum projection images of each brain.

Received 23 March; accepted 11 August 2004; doi:10.1038/nature02926.

1. Dunlap, J. C. Molecular bases for circadian clocks. *Cell* **96,** 271–290 (1999).
2. Panda, S., Hogenesch, J. & Kay, S. Circadian rhythms from flies to human. *Nature* **417,** 329–335 (2002).
3. Wheeler, D. A., Hamblen-Coyle, M. J., Dushay, M. S. & Hall, J. C. Behavior in light-dark cycles of *Drosophila* mutants that are arrhythmic, blind, or both. *J. Biol. Rhythms* **8,** 67–94 (1993).
4. Helfrich-Forster, C. Differential control of morning and evening components in the activity rhythm of *Drosophila melanogaster*—sex specific differences suggest a different quality of activity. *J. Biol. Rhythms* **2,** 135–154 (2000).
5. Hall, J. Genetics and molecular biology of rhythms in *Drosophila* and other insects. *Adv. Genet.* **48,** 1–280 (2003).
6. Pittendrigh, C. S. & Daan, S. A functional analysis of circadian pacemakers in nocturnal rodents. V. Pacemaker structure: A clock for all seasons. *J. Comp. Physiol.* **106,** 333–355 (1976).
7. Helfrich-Forster, C. The locomotor activity rhythm of *Drosophila melanogaster* is controlled by a dual oscillator system. *J. Insect Physiol.* **47,** 877–887 (2001).
8. Kaneko, M. & Hall, J. C. Neuroanatomy of cells expressing clock genes in *Drosophila*: Transgenic manipulation of the period and timeless genes to mark the perikarya of circadian pacemaker neurons and their projections. *J. Comp. Neurol.* **422,** 66–94 (2000).
9. Helfrich-Forster, C. The Period clock gene is expressed in central nervous system neurons which also produce a neuropeptide that reveals the projections of circadian pacemaker cells within the brain of *Drosophila melanogaster*. *Proc. Natl Acad. Sci. USA* **92,** 612–616 (1995).
10. Renn, S. C. P., Park, J. H., Rosbash, M., Hall, J. C. & Taghert, P. H. A *pdf* neuropeptide gene mutation and ablation of PDF neurons each cause severe abnormalities of behavioral circadian rhythms in *Drosophila*. *Cell* **99,** 791–802 (1999).
11. Park, J. H. *et al.* Differential regulation of circadian pacemaker output by separate clock genes in *Drosophila*. *Proc. Natl Acad. Sci. USA* **97,** 3608–3613 (2000).
12. Peng, Y., Stoleru, D., Levine, J. D., Hall, J. C. & Rosbash, M. *Drosophila* free-running rhythms require intercellular communication. *PLoS Biol.* **1,** E13 (2003).
13. Emery, P. *et al. Drosophila* CRY is a deep brain circadian photoreceptor. *Neuron* **26,** 493–504 (2000).
14. Klarsfeld, A. *et al.* Novel features of cryptochrome-mediated photoreception in the brain circadian clock of *Drosophila*. *J. Neurosci.* **24,** 1468–1477 (2004).
15. Zhao, J. *et al. Drosophila* clock can generate ectopic circadian clocks. *Cell* **113,** 755–766 (2003).
16. Rao, S., Lang, C., Levitan, E. S. & Deitcher, D. L. Visualization of neuropeptide expression, transport, and exocytosis in *Drosophila melanogaster*. *J. Neurobiol.* **49,** 159–172 (2001).
17. Blanchardon, E. *et al.* Defining the role of *Drosophila* lateral neurons in the control of circadian rhythms in motor activity and eclosion by targeted genetic ablation and PERIOD protein overexpression. *Eur. J. Neurosci.* **13,** 871–888 (2001).
18. Veleri, S., Brandes, C., Helfrich-Forster, C., Hall, J. C. & Stanewsky, R. A self-sustaining, light-entrainable circadian oscillator in the *Drosophila* brain. *Curr. Biol.* **13,** 1758–1767 (2003).
19. Lee, T. & Luo, L. Mosaic analysis with a repressible cell marker for studies of gene function in neuronal morphogenesis. *Neuron* **22,** 451–461 (1999).
20. Hardin, P. E., Hall, J. C. & Rosbash, M. Feedback of the *Drosophila period* gene product on circadian cycling of its messenger RNA levels. *Nature* **343,** 536–540 (1990).
21. Yang, Z. & Sehgal, A. Role of molecular oscillations in generating behavioral rhythms in *Drosophila*. *Neuron* **29,** 453–467 (2001).
22. Lee, H. S., Billings, H. J. & Lehman, M. N. The suprachiasmatic nucleus: a clock of multiple components. *J. Biol. Rhythms* **18,** 435–449 (2003).
23. Jagota, A., de la Iglesia, H. O. & Schwartz, W. J. Morning and evening circadian oscillations in the suprachiasmatic nucleus *in vitro*. *Nature Neurosci.* **3,** 372–376 (2000).
24. de la Iglesia, H. O., Meyer, J., Carpino, A. Jr & Schwartz, W. J. Antiphase oscillation of the left and right suprachiasmatic nuclei. *Science* **290,** 799–801 (2000).
25. Yamaguchi, S. *et al.* Synchronization of cellular clocks in the suprachiasmatic nucleus. *Science* **302,** 1408–1412 (2003).
26. Yoshii, T. *et al. Drosophila* cry(b) mutation reveals two circadian clocks that drive locomotor rhythm and have different responsiveness to light. *J. Insect Physiol.* **50,** 479–488 (2004).
27. Harmar, A. *et al.* The VPAC(2) receptor is essential for circadian function in the mouse suprachiasmatic nuclei. *Cell* **109,** 497–508 (2002).
28. Nitabach, M. N., Blau, J. & Holmes, T. C. Electrical silencing of *Drosophila* pacemaker neurons stops the free-running circadian clock. *Cell* **109,** 485–495 (2002).
29. Levine, J., Funes, P., Dowse, H. & Hall, J. Signal analysis of behavioral and molecular cycles. *BMC Neurosci.* **3,** 1 (2002).
30. Levine, J., Funes, P., Dowse, H. & Hall, J. Advanced analysis of a cryptochrome mutation's effects on the robustness and phase of molecular cycles in isolated peripheral tissues of *Drosophila*. *BMC Neurosci.* **3,** 5 (2002).
31. Grima, B., Chélot, E., Xia, R. & Rouyer, F. Morning and evening activity peaks are controlled by different clock neurons of the *Drosophila* brain. *Nature* doi:10.1038/nature02935 (this issue).

Supplementary Information accompanies the paper on **www.nature.com/nature**.

Acknowledgements We thank A. Sehgal for providing the *UAS-per2-4* flies and L. Luo for tubulinP-*GAL80* plasmid, as well as J. Levine, R. Allada, L. Griffith, P. Emery and M.R. laboratory members for discussion and critical comments on the manuscript. We are grateful to J. Hall, P. Nawathean and M. McDonald for their support and advice. We also thank E. Dougherty for assistance in confocal microscopy, and H. Felton for administrative assistance. The work was supported in part by grants from the NIH to M.R.

Competing interests statement The authors declare that they have no competing financial interests.

Correspondence and requests for materials should be addressed to M.R. (rosbash@brandeis.edu).